

TRIUMF	UNIVERSITY OF ALBERTA EDMONTON, ALBERTA	
	Date 1998/01/13	File No. TRI-DNA-98-1
Author GM Stinson		Page 1 of 21
Subject Revised extraction data for beam line 2A		

1. Introduction

An earlier report¹⁾ listed extraction data for beam line 2A. That data was used to develop an analytic expression for the field setting of the combination magnet of the beam line. In addition, the fringe-field extraction parameters were listed.

Since that report was issued, it was found that the values of the fringe field parameters oscillated somewhat and a request was made of R. Lee to see if a revised set of extraction parameters could be obtained. He provided a revised set of extraction parameters in December of 1997²⁾ and these were used to recalculate the optics of the beam line.

The data presented in this report are the revised calculations and, as such, data presented here supercedes that presented in ref¹⁾.

2. Extraction data

The revised extraction parameters for beam line 2A provided by R. Lee cover an energy range from 470 MeV to 510 MeV. Table 1 lists the stripping radius and angle and the combination magnet field that were obtained in the revised calculations. The rightmost column of the table gives an estimate of the current required to produce the calculated field. We include the following relevant subsections from ref¹⁾ for completeness.

2.1 Analysis of the field versus energy extraction data

The program PLOTDATA³⁾ was used to fit the calculated combination magnet fields to expressions that were linear, quadratic and cubic function of the extracted energy. The results of the fits are given below; in the expressions, the field B is given in kG for energies E in MeV.

Type of fit	Fitted expression
Linear	$B = 73.66786 - 14.98534 \left[\frac{E}{100} \right]$
Quadratic	$B = 62.05789 - 10.24381 \left[\frac{E}{100} \right] - 0.4838294 \left[\frac{E}{100} \right]^2$
Cubic	$B = 1153.09 - 678.6901 \left[\frac{E}{100} \right] + 135.9815 \left[\frac{E}{100} \right]^2 - 9.283356 \left[\frac{E}{100} \right]^3$

Figures 1, 2 and 3 show the linear, quadratic and cubic fits, respectively, to the calculated data. On the scales presented there is little difference to be seen. However, as shown in figure 4—a plot of the *differences* between the calculated and fitted fields—the cubic fit is the best (as one should expect).

From the above expressions the energy at which the combination magnet field reverses is calculated to be 491.600 MeV from the linear fit, 491.644 MeV from the quadratic fit and 491.671 MeV from the cubic fit.

From this analysis it is recommended that the cubic fit to the 2A combination fields be used. The calculated and fitted fields are listed in table 2.

2.2 Measured field data

Measurement of the B - I data for the combination magnet was done by D. Evans in early 1997⁴⁾. The raw data collected by him is reproduced in the leftmost two columns of table 3. Figure 5 is a plot of this raw data. PLOTDATA was again used to fit this data as linear, quadratic and cubic functions of current. The following expressions were obtained for the three functional forms.

Type of fit	Fitted expression
Linear	$B = 0.1505329 + 1.852974 \left[\frac{I}{100} \right]$
Quadratic	$B = -0.1502813 + 2.149066 \left[\frac{I}{100} \right] - 0.05459045 \left[\frac{I}{100} \right]^2$
Cubic	$B = 0.05394736 + 1.80503 \left[\frac{I}{100} \right] + 0.09241018 \left[\frac{I}{100} \right]^2 - 0.01781268 \left[\frac{I}{100} \right]^3$

with B in kG and I in Amperes. Table 4 lists the results of the fits and figure 6 shows the cubic fit to the data.

Because the energy range of extraction is between 470 MeV and 510 MeV the ‘useful’ range of combination magnet fields lies between ± 4 kG. The data listed in the rightmost two columns of table 3 correspond to this energy range. Figure 7 is a plot of this field-current relationship. The data was then fitted to give more accurate predictions of the fields in the energy range of interest, again using PLOTDATA to obtain expressions for the fields as linear, quadratic and cubic functions of current. The resulting expressions are listed below.

Type of fit	Fitted expression
Linear	$B = -0.0157272 + 1.957545 \left[\frac{I}{100} \right]$
Quadratic	$B = -0.03624995 + 1.995333 \left[\frac{I}{100} \right] - 0.01433335 \left[\frac{I}{100} \right]^2$
Cubic	$B = -0.1340001 + 2.305834 \left[\frac{I}{100} \right] - 0.29800038 \left[\frac{I}{100} \right]^2 + 0.07666675 \left[\frac{I}{100} \right]^3$

with B in kG and I in Amperes. Table 5 lists the results of the fits and figure 8 shows the quadratic fit to the data.

In order to generate an estimate of the current required to produce a given field, PLOTDATA was used to invert the above relationships. The fits obtained are listed at the top of the next page with the current I in amperes and the *absolute value* of the field B in kG. It is the *cubic* fit that is listed as the combination magnet current in table 1.

3. Revised fringe-field parameters

Table 6 lists the revised transfer matrix elements in units suitable for use in the program TRANSPORT⁵⁾. As an indication of the difference between the previous and recalculated values, figures 9 and 10 show the

Type of fit	Fitted expression
Linear	$I = 100 [0.00823275 + 0.5107673 B]$
Quadratic	$I = 100 [0.01804125 + 0.501439 B + 0.00182142 B^2]$
Cubic	$I = 100 [0.06990472 + 0.415772 B + 0.0422539 B^2 - 0.005627461 B^3]$

values of R_{11} and R_{12} , respectively, of the recalculated and original parameters over the energy range of extraction. Recalculated values are shown as diamonds and the original values are plotted as a dotted line. The oscillations of the previous extraction parameters are readily apparent. In particular, the values of R_{11} have a peak-to-peak variation of approximately a factor of five. Those of R_{12} have a peak-to-peak variation of approximately 1%. The values of the recalculated parameters are seen to lie on a (relatively) smooth line.

Similar plots for R_{21} and R_{22} are shown in figures 11 and 12 where again oscillations are apparent in the original parameters with a peak-to-peak variation of R_{21} and R_{22} of approximately 1.5% and 2% respectively. The recalculated parameters are seen to lie on relatively smooth curves.

The dispersion parameters R_{16} and R_{26} are plotted in figures 13 and 14. These do not differ significantly between the two calculations. It is seen that, in both calculations, the values of the parameters could almost be said to lie on two different curves. The reason for this is unknown.

Plots of the vertical parameters R_{33} and R_{34} are shown in figures 15 and 16. Here it is seen that these parameters are the same in both calculations. R_{33} values lie on a smooth curve whereas the R_{34} values have discrete jumps as a function of energy. However, in the latter case these jumps are of the order of one part in six hundred and, as such, do not cause any significant problem.

Figures 17 and 18 show similar data for the parameters R_{43} and R_{44} . Here it is seen that there is little difference between the two calculations in the values of these parameters.

References

1. G. M. Stinson, *Extraction data for beam line 2A*, TRI-DNA-97-2, TRIUMF, February, 1997.
2. R. Lee, *Private communication*, TRIUMF, December 10, 1997.
3. J. L. Chuma, *Plotdata Command Reference Manual*, TRIUMF Report TRI-CD-87-03b, TRIUMF, June 1991.
4. D. Evans, *Private communication*, TRIUMF, March, 1997.
5. K. L. Brown, F. Rothacker, D. C. Carey and Ch. Iselin, *TRANSPORT, A Computer Program for Designing Charged Particle Beam Transport Systems*, CERN Report CERN 80-04, CERN, 1980.

Table 1
Stripping radius and angle and calculated combination magnet fields and currents for beam line 2A

Energy (MeV)	Stripping coordinates		Combination magnet field (kG)	Combination magnet current (A)
	Radius (in.)	θ ($^{\circ}$)		
470	300.137	306.413	3.24704	167.279
471	300.141	306.576	3.09329	159.377
472	300.146	306.739	2.94113	151.510
473	300.150	306.900	2.78680	143.495
474	300.154	307.060	2.63448	135.563
475	300.158	307.219	2.48425	127.729
476	300.162	307.379	2.33002	119.689
477	300.166	307.539	2.17732	111.742
478	300.170	307.696	2.02744	103.966
479	300.174	307.852	1.87581	96.136
480	300.177	308.008	1.72584	88.440
481	300.181	308.163	1.57662	80.840
482	300.185	308.317	1.42645	73.263
483	300.189	308.470	1.27745	65.826
484	300.192	308.621	1.13126	58.618
485	300.195	308.771	0.98253	51.387
486	300.199	308.922	0.83537	44.344
487	300.202	309.071	0.68998	37.505
488	300.205	309.221	0.54102	30.633
489	300.208	309.370	0.39516	24.045
490	300.211	309.520	0.24779	17.544
491	300.215	309.670	0.09830	11.118
492	300.218	309.819	-0.04883	-9.031
493	300.221	309.969	-0.19727	-15.353
494	300.224	310.118	-0.34632	-21.873
495	300.227	310.267	-0.49428	-28.506
496	300.230	310.417	-0.64355	-35.348
497	300.233	310.565	-0.79346	-42.360
498	300.237	310.715	-0.94312	-49.490
499	300.240	310.864	-1.09280	-56.738
500	300.243	311.013	-1.24456	-64.196

Table 1 (Continued)

Stripping radius and angle and calculated combination magnet fields and currents for beam line 2A

Energy (MeV)	Stripping coordinates		Combination magnet field (kG)	Combination magnet current (A)
	Radius (in.)	θ ($^{\circ}$)		
501	300.246	311.162	-1.39349	-71.611
502	300.250	311.311	-1.54458	-79.218
503	300.252	311.463	-1.69744	-86.988
504	300.255	311.615	-1.85137	-94.878
505	300.258	311.770	-2.00631	-102.878
506	300.264	311.921	-2.16272	-110.982
507	300.268	312.074	-2.31634	-118.976
508	300.271	312.230	-2.47797	-127.402
509	300.276	312.389	-2.63902	-135.800
510	300.280	312.552	-2.80377	-144.378

Table 2

Comparison of the calculated and fitted combination magnet fields

Energy (MeV)	B (kG) Ref ¹	B (kG)		
		(Linear fit)	(Quadratic fit)	(Cubic fit)
470	3.24704	3.23676	3.22420	3.25201
471	3.09329	3.08691	3.07623	3.09576
472	2.94113	2.93706	2.92817	2.94049
473	2.78680	2.78720	2.78000	2.78595
474	2.63448	2.63735	2.63175	2.63257
475	2.48425	2.48750	2.48339	2.47992
476	2.33002	2.33764	2.33494	2.32788
477	2.17732	2.18779	2.18640	2.17651
478	2.02744	2.03793	2.03775	2.02600
479	1.87581	1.88808	1.88901	1.87567
480	1.72584	1.73823	1.74017	1.72620
481	1.57662	1.58838	1.59124	1.57703
482	1.42645	1.43852	1.44221	1.42810
483	1.27745	1.28867	1.29308	1.28003
484	1.13126	1.13882	1.14386	1.13220
485	0.98253	0.98896	0.99454	0.98413
486	0.83537	0.83910	0.84512	0.83667
487	0.68998	0.68925	0.69561	0.68896
488	0.54102	0.53940	0.54599	0.54163
489	0.39516	0.38955	0.39629	0.39404
490	0.24779	0.23969	0.24648	0.24658
491	0.09830	0.08984	0.09658	0.09912
492	-0.04883	-0.06001	-0.05342	-0.04871
493	-0.19727	-0.20986	-0.20351	-0.19641
494	-0.34632	-0.35972	-0.35371	-0.34460
495	-0.49428	-0.50957	-0.50399	-0.49304
496	-0.64355	-0.65942	-0.65438	-0.64197
497	-0.79346	-0.80927	-0.80486	-0.79150
498	-0.94312	-0.95913	-0.95544	-0.94141
499	-1.09280	-1.10898	-1.10612	-1.09180
500	-1.24456	-1.25884	-1.25689	-1.24268

Table 2 (Continued)

Comparison of the calculated and fitted combination magnet fields

Energy (MeV)	B (kG) Ref ¹	B (kG)		
		(Linear fit)	(Quadratic fit)	(Cubic fit)
501	-1.39349	-1.40870	-1.40776	-1.39429
502	-1.54458	-1.55855	-1.55873	-1.54651
503	-1.69744	-1.70840	-1.70979	-1.69983
504	-1.85137	-1.85825	-1.86095	-1.85352
505	-2.00631	-2.00811	-2.01221	-2.00830
506	-2.16272	-2.15796	-2.16356	-2.16394
507	-2.31634	-2.30782	-2.31501	-2.32056
508	-2.47797	-2.45766	-2.46655	-2.47852
509	-2.63902	-2.60752	-2.61820	-2.63733
510	-2.80377	-2.75737	-2.76994	-2.79736

Table 3

Measured combination magnet field as a function of current

Raw data		Useful range	
<i>I</i> (A)	Field (kG)	<i>I</i> (A)	Field (kG)
50	0.954	50	0.954
100	1.938	100	1.938
150	2.913	150	2.913
200	3.888	200	3.888
250	4.841	200	3.914
300	5.789	100	1.963
350	6.715		
400	7.612		
450	8.427		
500	9.146		
400	7.674		
300	5.824		
200	3.914		
100	1.963		

Table 4

Fitted values to the raw data for the 2A combination magnet field

I (A)	B_{meas} (kG)	Type of fit		
		Linear	Quadratic	Cubic
50	0.954	1.07702	0.91060	0.97734
100	1.938	2.00351	1.94419	1.93358
150	2.913	2.92999	2.95049	2.90930
200	3.884	3.85648	3.92949	3.89115
250	4.841	4.78297	4.88119	4.86576
300	5.789	5.70946	5.80560	5.81979
350	6.715	6.63594	6.70272	6.73986
400	7.612	7.56243	7.57254	7.61262
450	8.427	8.48892	8.41506	8.42471
500	9.146	9.41540	9.23029	9.16277
400	7.674	7.56243	7.57254	7.61262
300	5.824	5.70946	5.80560	5.81979
200	3.914	3.85648	3.92949	3.89115
100	1.963	2.00351	1.94419	1.93358

Table 5

Fitted values to the useful data for the 2A combination magnet field

I (A)	B_{meas} (kG)	Type of fit		
		Linear	Quadratic	Cubic
50	0.954	0.96305	0.95783	0.9540
100	1.938	1.94182	1.94475	1.9505
150	2.913	2.92059	2.92450	2.9130
200	3.884	3.89936	3.89708	3.8990
200	3.914	3.89936	3.89708	3.8990
100	1.963	1.94182	1.94475	1.9505

Table 6
Transfer matrix elements for beam line 2A

Energy (MeV)	Horizontal transfer matrix elements					
	R_{11} (cm/cm)	R_{12} (cm/mr)	R_{16} (cm/%)	R_{21} (mr/cm)	R_{22} (mr/mr)	R_{26} (mr/%)
470	-0.01938	0.333018	1.41816	-3.05430	0.17448	2.37640
471	-0.01985	0.332567	1.41315	-3.05560	0.17392	2.37860
472	-0.01362	0.331810	1.40749	-3.04250	0.17265	2.37920
473	-0.02049	0.330994	1.40333	-3.06030	0.17122	2.38320
474	-0.02086	0.330734	1.38757	-3.06310	0.17113	2.36020
475	-0.02129	0.330275	1.39543	-3.06530	0.17068	2.39160
476	-0.02126	0.329538	1.38925	-3.06560	0.16951	2.39120
477	-0.02160	0.329436	1.37422	-3.06780	0.16985	2.37000
478	-0.02265	0.329040	1.38053	-3.07160	0.16942	2.39750
479	-0.02219	0.328514	1.37574	-3.07180	0.16876	2.39980
480	-0.02257	0.328475	1.36150	-3.07450	0.16920	2.38040
481	-0.02310	0.328181	1.36757	-3.07630	0.16917	2.40710
482	-0.02300	0.327777	1.36115	-3.07570	0.16884	2.40560
483	-0.02410	0.327828	1.34868	-3.07570	0.16958	2.38970
484	-0.02196	0.327590	1.35484	-3.07590	0.16960	2.41610
485	-0.02238	0.327225	1.34963	-3.07790	0.16938	2.41700
486	-0.02217	0.326875	1.33633	-3.07880	0.16916	2.39940
487	-0.02150	0.327163	1.34164	-3.07840	0.17053	2.42340
488	-0.02180	0.326804	1.33730	-3.07930	0.17032	2.42610
489	-0.02311	0.326587	1.33255	-3.08320	0.17042	2.42770
490	-0.02322	0.326659	1.32879	-3.08430	0.17120	2.43140
491	-0.02404	0.323020	1.34590	-3.08650	0.17104	2.43460
492	-0.02454	0.361030	1.22980	-3.08880	0.17119	2.44340
493	-0.02670	0.326050	1.31600	-3.09310	0.17182	2.44060
494	-0.02779	0.325650	1.31190	-3.09510	0.17160	2.44360
495	-0.02978	0.325360	1.30810	-3.09880	0.17160	2.44710
496	-0.03137	0.325260	1.30250	-3.10250	0.17210	2.44700
497	-0.03196	0.324830	1.29960	-3.10410	0.17190	2.45250
498	-0.03389	0.324470	1.29570	-3.10860	0.17180	2.45600
499	-0.03543	0.324338	1.29175	-3.11200	0.17231	2.45940
500	-0.03717	0.323894	1.28344	-3.11530	0.17220	2.45410

Table 6 (Continued)
Transfer matrix elements for beam line 2A

Energy (MeV)	Horizontal transfer matrix elements					
	R_{11} (cm/cm)	R_{12} (cm/mr)	R_{16} (cm/%)	R_{21} (mr/cm)	R_{22} (mr/mr)	R_{26} (mr/%)
501	-0.03685	0.323606	1.28355	-3.11450	0.17228	2.46520
502	-0.03801	0.323491	1.27943	-3.11700	0.17281	2.46820
503	-0.04033	0.323044	1.27514	-3.12170	0.17258	2.47050
504	-0.04437	0.322603	1.26301	-3.13040	0.17240	2.45630
505	-0.04374	0.322609	1.26652	-3.12880	0.17322	2.47630
506	-0.04607	0.322181	1.26233	-3.13280	0.17328	2.47980
507	-0.04879	0.322060	1.25807	-3.13730	0.17390	2.48250
508	-0.05819	0.321357	1.23957	-3.15670	0.17325	2.45540
509	-0.05526	0.321165	1.24952	-3.14980	0.17378	2.48880
510	-0.05904	0.320807	1.24010	-3.15670	0.17402	2.48220

Table 6 (Continued)
Transfer matrix elements for beam line 2A

Energy (MeV)	Vertical transfer matrix elements			
	R_{33} (cm/cm)	R_{34} (cm/mr)	R_{43} (mr/cm)	R_{44} (mr/mr)
470	1.13384	0.622629	0.47860	1.14480
471	1.13350	0.622692	0.47980	1.14582
472	1.13385	0.622872	0.48260	1.14707
473	1.13271	0.622784	0.48160	1.14763
474	1.13106	0.619960	0.48320	1.14898
475	1.12979	0.619842	0.48160	1.14937
476	1.12954	0.619895	0.48250	1.15011
477	1.12885	0.619861	0.48210	1.15057
478	1.12752	0.619721	0.48010	1.15077
479	1.12706	0.619724	0.48010	1.15124
480	1.12664	0.619845	0.48200	1.15277
481	1.12510	0.619659	0.47910	1.15268
482	1.12426	0.619583	0.47780	1.15281
483	1.12378	0.619568	0.47740	1.15305
484	1.12225	0.619381	0.47430	1.15284
485	1.12121	0.619273	0.47230	1.15276
486	1.11973	0.616431	0.47310	1.15351
487	1.11812	0.616255	0.46970	1.15322
488	1.11726	0.616142	0.46780	1.15301
489	1.11681	0.616097	0.46690	1.15295
490	1.11565	0.615927	0.46410	1.15254
491	1.11498	0.615824	0.46230	1.15223
492	1.11429	0.615832	0.46230	1.15292
493	1.11395	0.615779	0.46130	1.15268
494	1.11310	0.615636	0.45890	1.15218
495	1.11220	0.615489	0.45640	1.15163
496	1.11180	0.615398	0.45480	1.15118
497	1.11130	0.615300	0.45310	1.15066
498	1.11060	0.615151	0.45070	1.14998
499	1.10912	0.612189	0.44980	1.14989
500	1.10838	0.612023	0.44710	1.14908

Table 6 (Continued)
Transfer matrix elements for beam line 2A

Energy (MeV)	Vertical transfer matrix elements			
	R_{33} (cm/cm)	R_{34} (cm/mr)	R_{43} (mr/cm)	R_{44} (mr/mr)
501	1.10815	0.611940	0.44560	1.14846
502	1.10770	0.611812	0.44340	1.14767
503	1.10710	0.611658	0.44080	1.14682
504	1.10663	0.611519	0.43850	1.14595
505	1.10676	0.611576	0.43910	1.14617
506	1.10600	0.611372	0.43560	1.14495
507	1.10542	0.611209	0.43270	1.14386
508	1.10489	0.611009	0.42960	1.14266
509	1.10461	0.610834	0.42700	1.14144
510	1.10405	0.610608	0.42360	1.14005

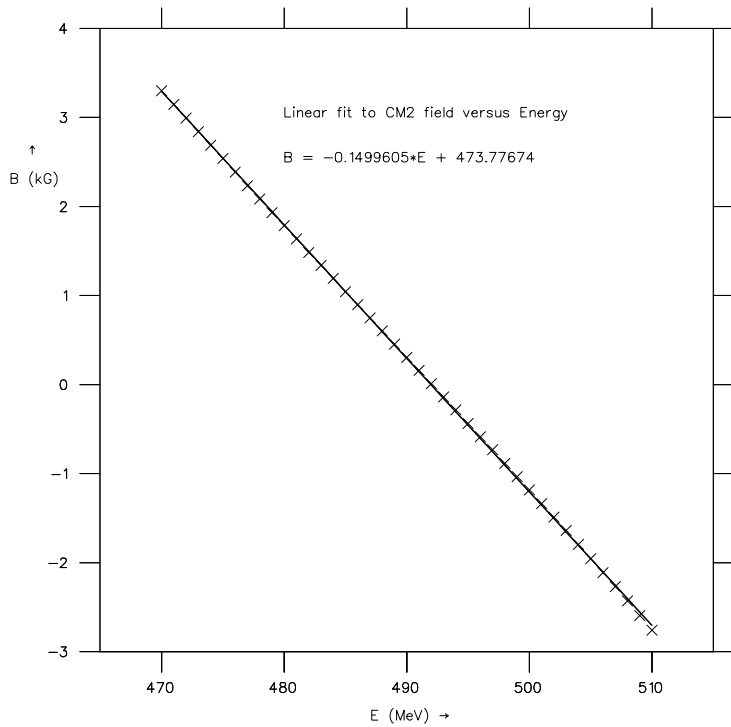


Fig. 1. Linear fit to 2A combination magnet field.

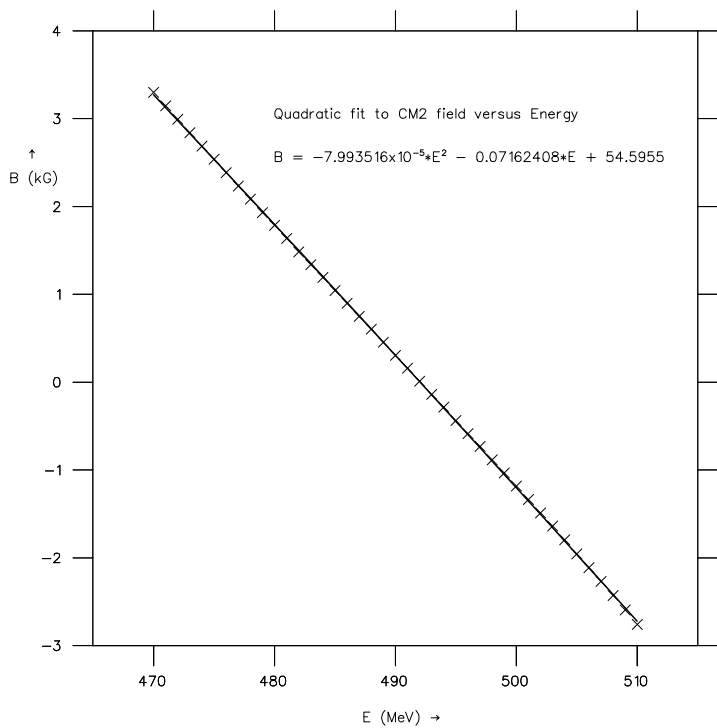


Fig. 2. Quadratic fit to 2A combination magnet field.

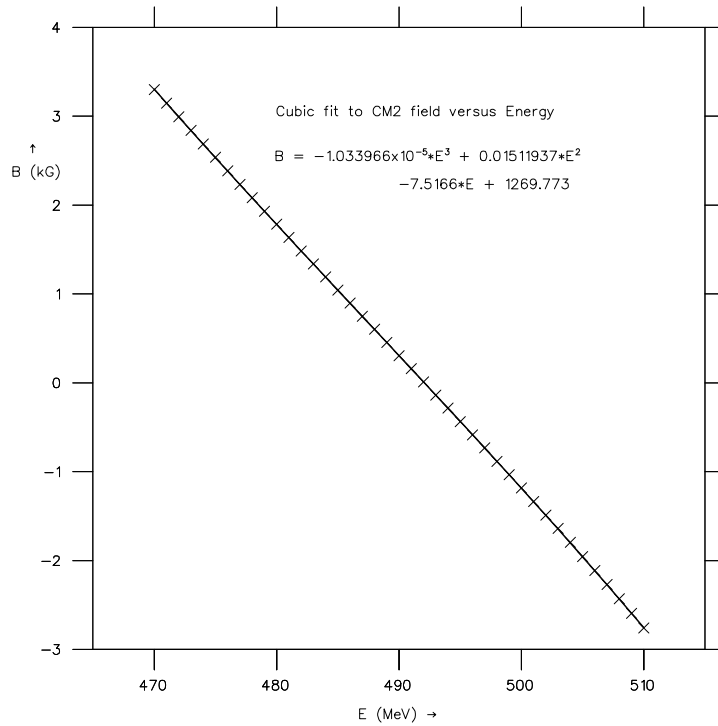


Fig. 3. Cubic fit to 2A combination magnet field.

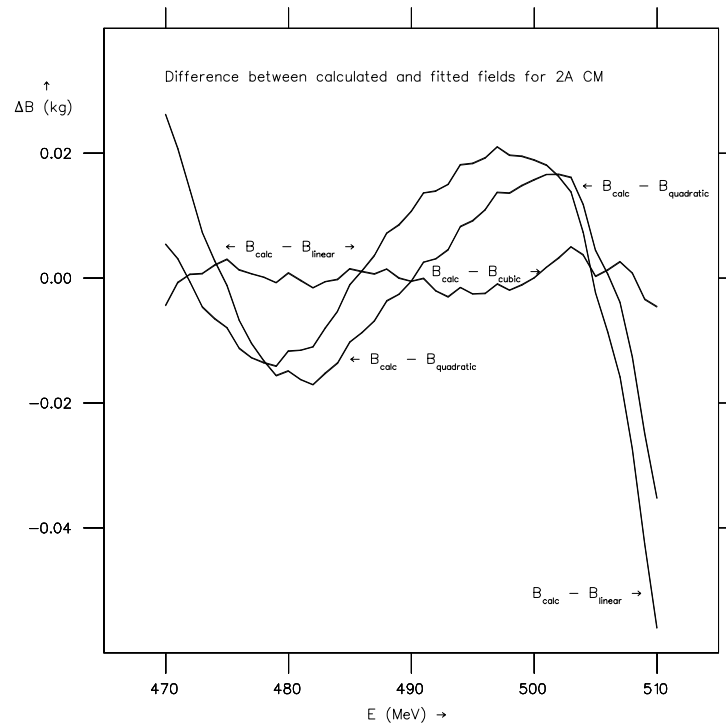
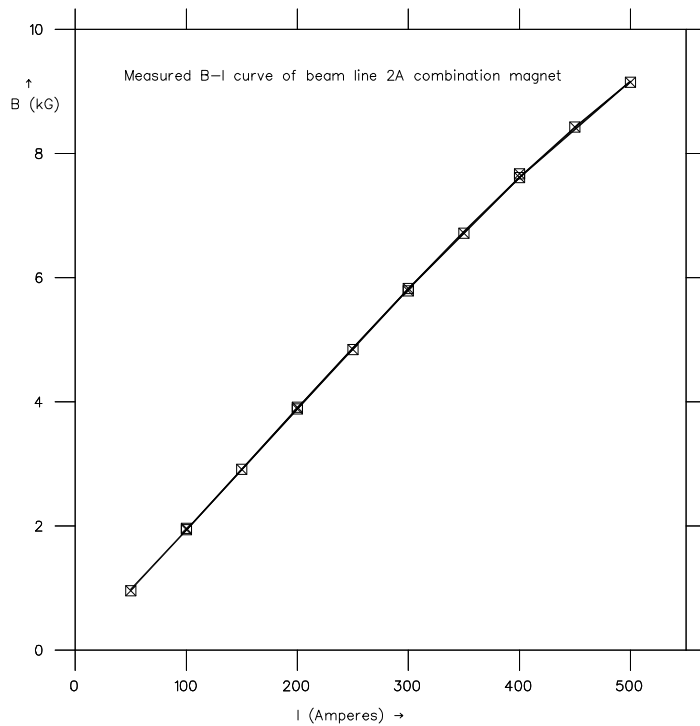
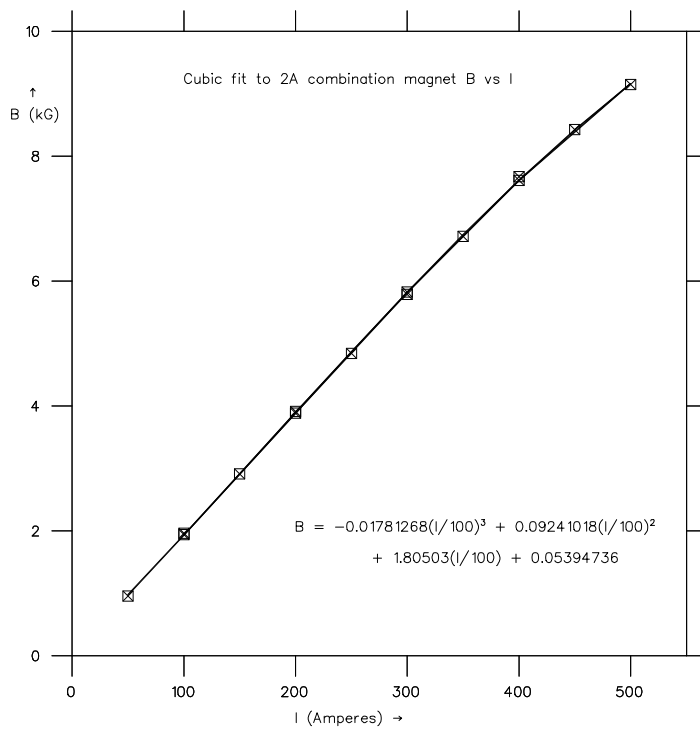


Fig. 4. Difference between calculated and fitted fields for 2A combination magnet.

Fig. 5. Plot of the raw B - I measured data of the 2A combination magnet.Fig. 6. Cubic fit to the raw B - I measured data of the 2A combination magnet.

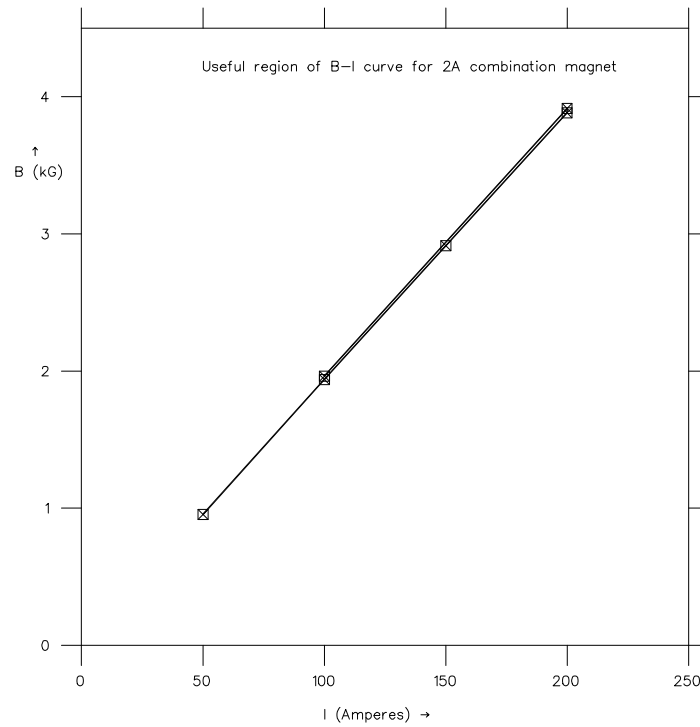


Fig. 7. Plot of the useful range of B - I measured data of the 2A combination magnet.

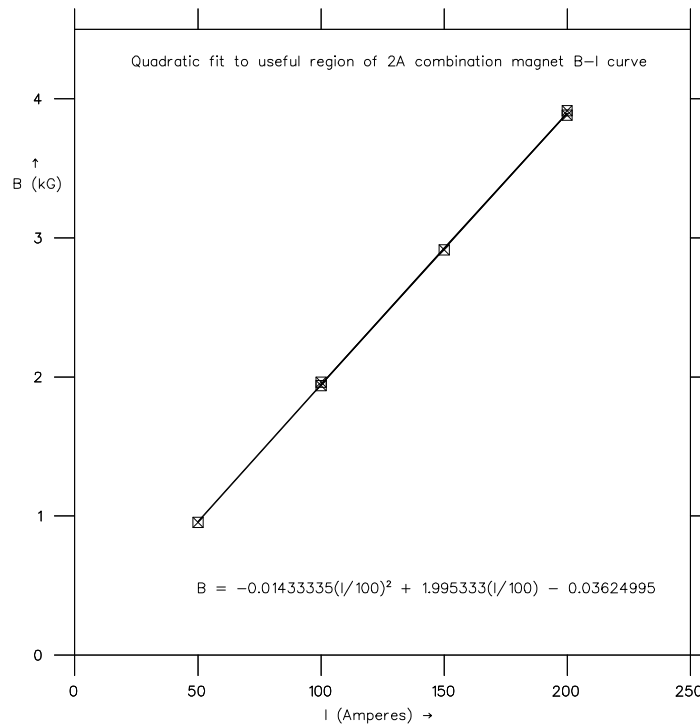
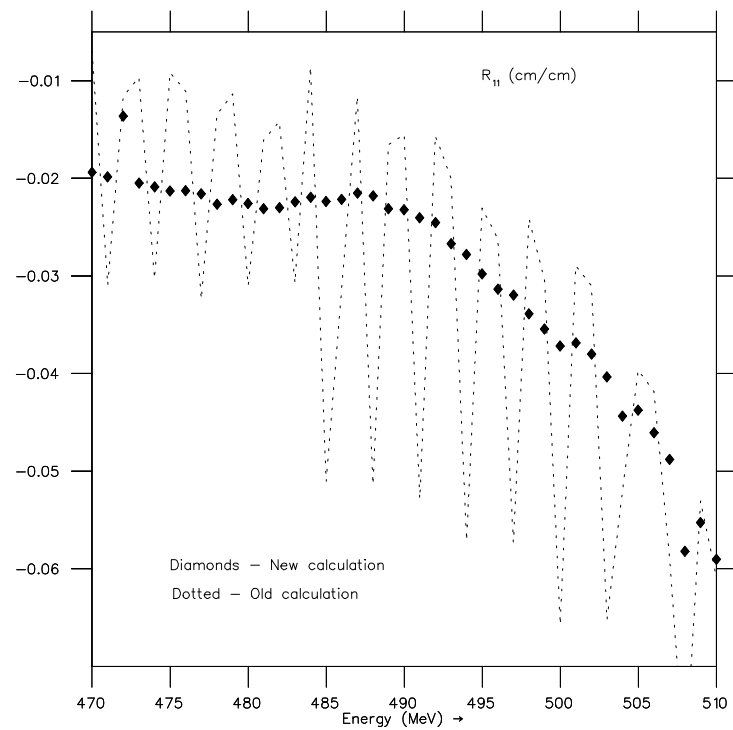
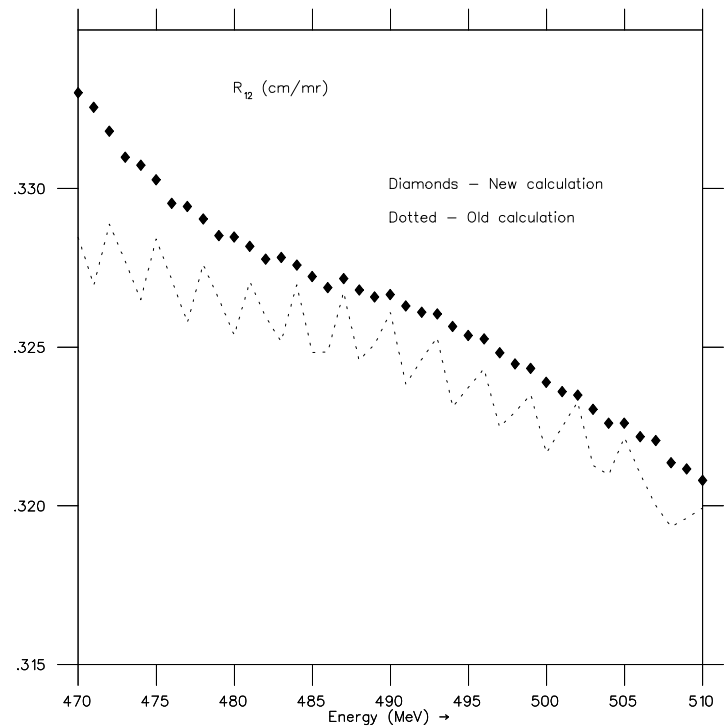


Fig. 8. Quadratic fit to the useful range of B - I measured data of the 2A combination magnet.

Fig. 9. Plot of the recalculated (diamonds) and original (dotted) values of R_{11} .Fig. 10. Plot of the recalculated (diamonds) and original (dotted) values of R_{12} .

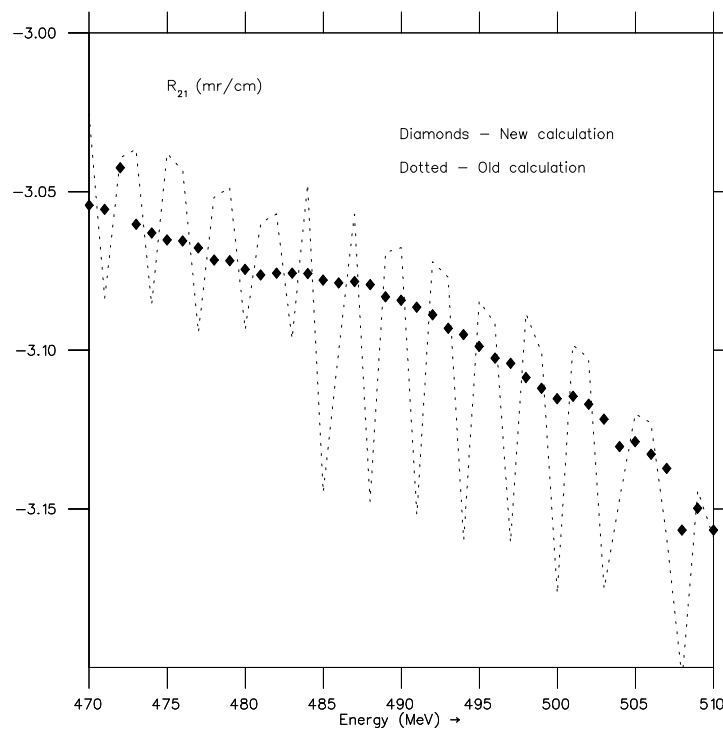


Fig. 11. Plot of the recalculated (diamonds) and original (dotted) values of R_{21} .

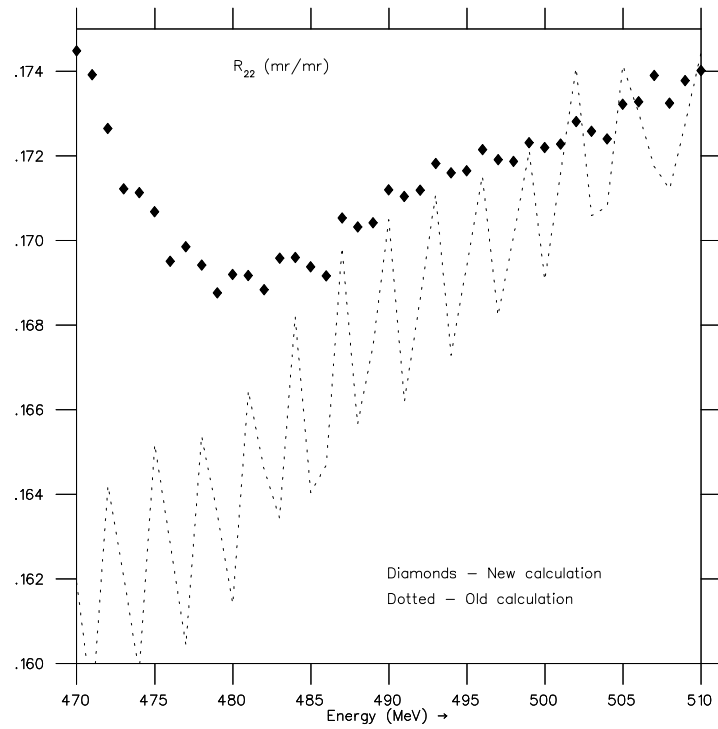
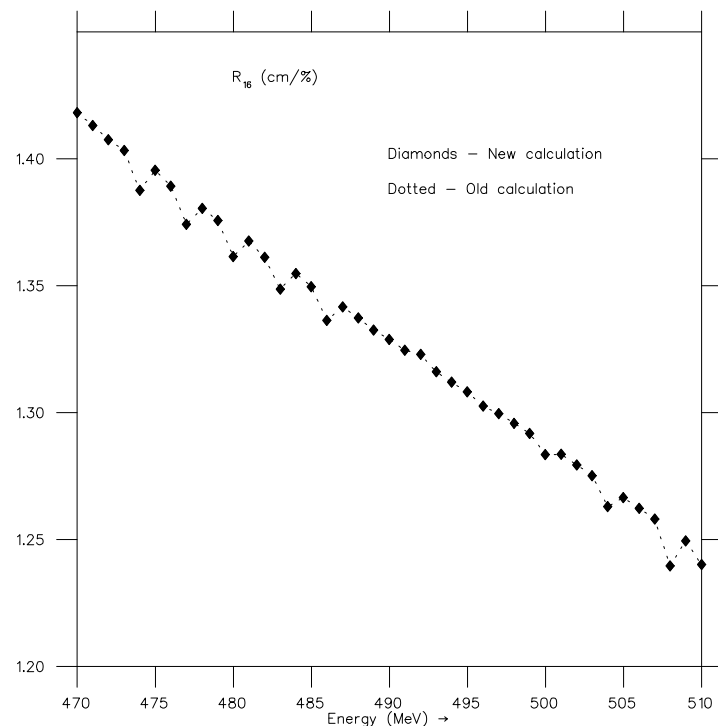
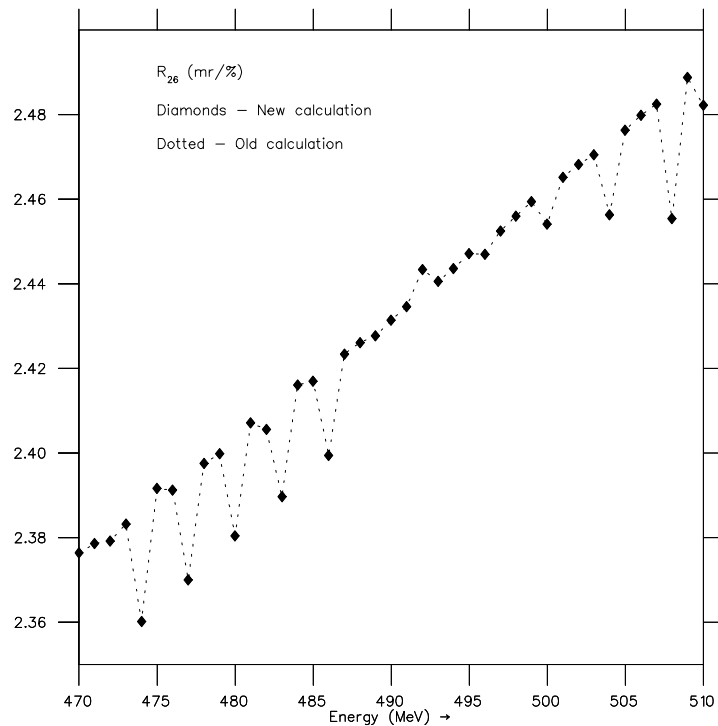
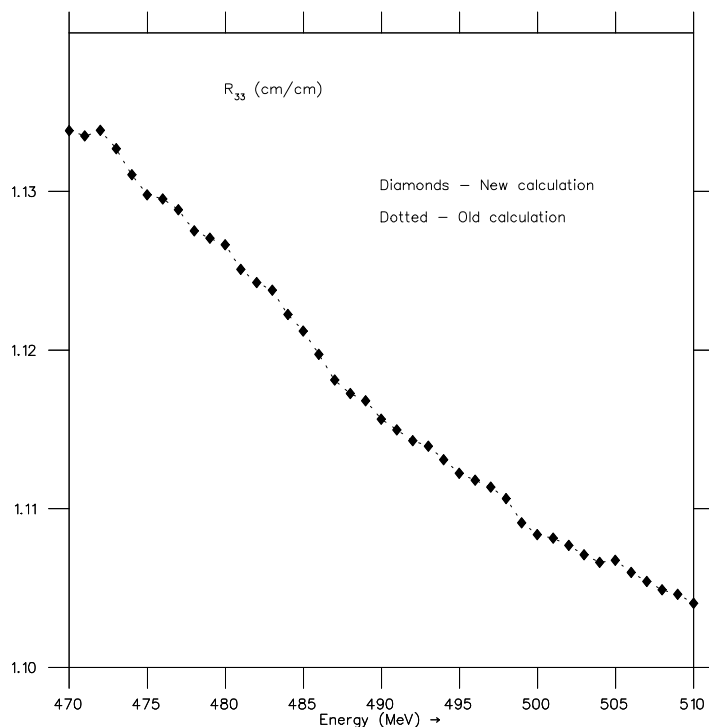
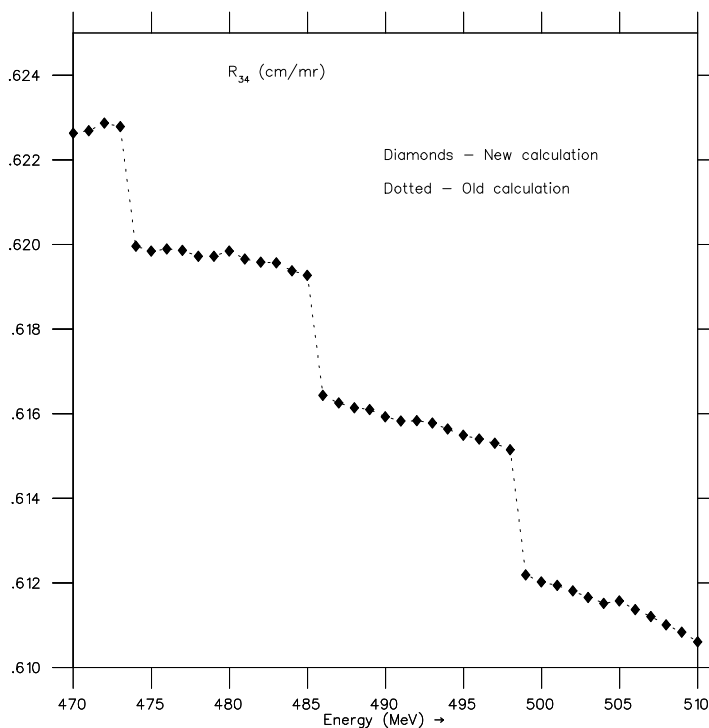
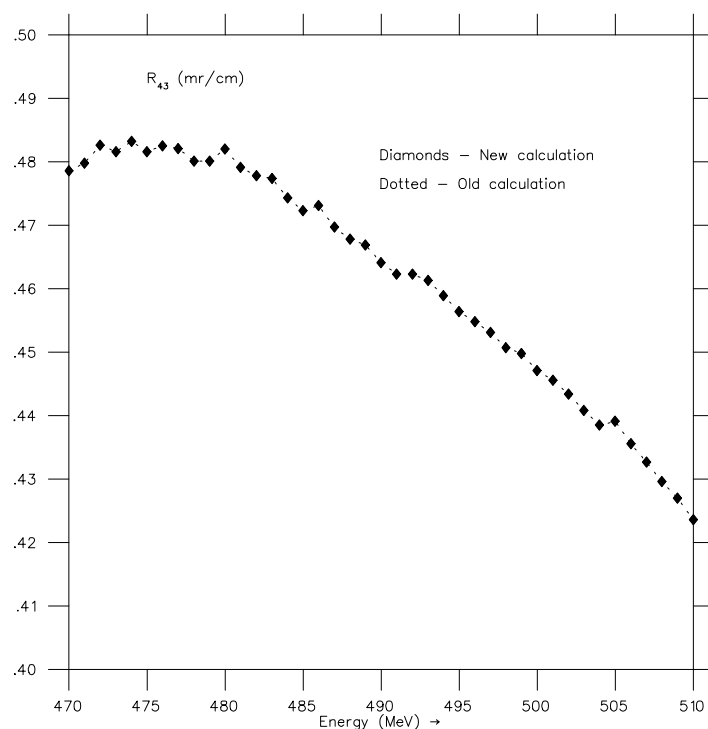
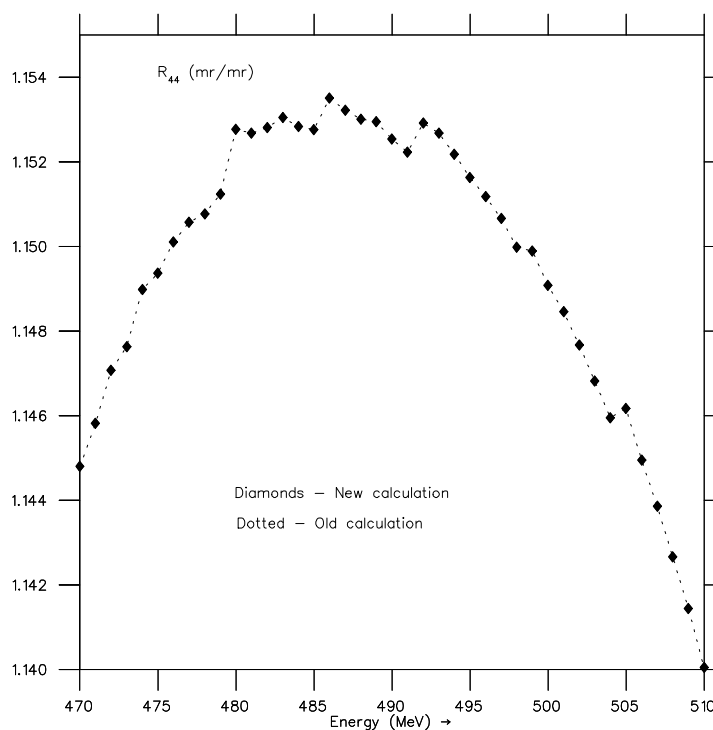


Fig. 12. Plot of the recalculated (diamonds) and original (dotted) values of R_{22} .

Fig. 13. Plot of the recalculated (diamonds) and original (dotted) values of R_{16} .Fig. 14. Plot of the recalculated (diamonds) and original (dotted) values of R_{26} .

Fig. 15. Plot of the recalculated (diamonds) and original (dotted) values of R_{33} .Fig. 16. Plot of the recalculated (diamonds) and original (dotted) values of R_{34} .

Fig. 17. Plot of the recalculated (diamonds) and original (dotted) values of R_{43} .Fig. 18. Plot of the recalculated (diamonds) and original (dotted) values of R_{44} .